

## How an Inhibitor of the HIV-I Protease Modulates Proteasome Activity\*

(Received for publication, July 23, 1999, and in revised form, September 23, 1999)

Gunter Schmidtke‡, Hermann-Georg Holzhütter§, Matthew Bogyo¶, Norman Kairies||, Michael Groll||, Rita de Giuli‡, Sabine Emch‡, and Marcus Groettrup‡\*\*

From the ‡Research Department, Cantonal Hospital St. Gall, CH-9007 St. Gallen, Switzerland, the §Institute for Biochemistry, Medical Faculty (Charité), Humboldt University, D-10117 Berlin, Germany, the ¶Department of Biochemistry and Biophysics, University of California, San Francisco, California 94143, and the ||Max Planck Institute for Biochemistry, D-82152 Martinsried, Germany

**The human immunodeficiency virus, type I protease inhibitor Ritonavir has been used successfully in AIDS therapy for 4 years. Clinical observations suggested that Ritonavir may exert a direct effect on the immune system unrelated to inhibition of the human immunodeficiency virus, type I protease. In fact, Ritonavir inhibited the major histocompatibility complex class I restricted presentation of several viral antigens at therapeutically relevant concentrations (5  $\mu$ M). In search of a molecular target we found that Ritonavir inhibited the chymotrypsin-like activity of the proteasome whereas the tryptic activity was enhanced. In this study we kinetically analyzed how Ritonavir modulates proteasome activity and what consequences this has on cellular functions of the proteasome. Ritonavir is a reversible effector of proteasome activity that protected the subunits MB-1 (X) and/or LMP7 from covalent active site modification with the vinyl sulfone inhibitor<sup>125</sup>I-NLVS, suggesting that they are the prime targets for competitive inhibition by Ritonavir. At low concentrations of Ritonavir (5  $\mu$ M) cells were more sensitive to canavanine but proliferated normally whereas at higher concentrations (50  $\mu$ M) protein degradation was affected, and the cell cycle was arrested in the G<sub>1</sub>/S phase. Ritonavir thus modulates antigen processing at concentrations at which vital cellular functions of the proteasome are not yet severely impeded. Proteasome modulators may hence qualify as therapeutics for the control of the cytotoxic immune response.**

The human immunodeficiency virus, type I (HIV-I)<sup>1</sup> encodes an aspartic endoprotease that is required for cleavage of the viral gag-pol polyprotein. Inhibition of the HIV-I protease leads to the release of noninfectious virus particles and has thus been the aim of drug development in AIDS therapy (1). Several cleavages performed by the HIV-I protease lie between the

amino acids phenylalanine (or tyrosine) and proline. Endoproteolytic cleavages N-terminal of proline residues have not been frequently observed in mammalian proteases, which was the premise for the design of transition state mimetics of the Phe-Pro bond as potential inhibitors of the HIV-I protease (2). Interestingly, an exception to this premise arose from the recent analysis of the cleavage specificity of the 20 S proteasome (3) that quite frequently cleaved polypeptide substrates N-terminal of proline residues (4–8).

A number of HIV-I protease inhibitors have been successfully used in clinical therapy of HIV-I infection (9). Patients treated with highly active antiretroviral therapy consisting of HIV-I protease inhibitors and nucleoside analogues showed a marked decrease in viremia with a simultaneous increase in CD4<sup>+</sup> helper T cells after the initiation of treatment. Remarkably, even in patients that (because of resistance of the virus) remained viremic upon highly active antiretroviral therapy, the number of CD4<sup>+</sup> helper T cells in peripheral blood increased suggesting that there was a direct effect of highly active antiretroviral therapy on the immune system unrelated to the inhibition of viral replication (10). This clinical finding was the incentive to test whether a widely applied HIV-I protease inhibitor named Ritonavir (11) would have an effect on the immune response in a well defined model system as, for instance, the infection of the mouse with lymphocytic choriomeningitis virus (LCMV). Surprisingly, the treatment of mice with therapeutical concentrations of Ritonavir markedly reduced the cytotoxic immune response against two T cell epitopes of LCMV and prevented the expansion of LCMV-reactive cytotoxic T cells (12). This effect was not because of an inhibition of LCMV replication but resulted from a decrease in the presentation of LCMV epitopes on major histocompatibility complex class I molecules of infected cells. In search of a potential molecular target for Ritonavir we tested its effect on peptide hydrolysis by the 20 S proteasome as it is the key enzyme for the generation of antigenic peptides as ligands for major histocompatibility complex class I molecules (3, 13).

Ritonavir inhibited the chymotryptic activity of mouse and human 20 S proteasomes at a similar potency as *N*-acetyl-leucyl-leucyl-norleucinal (LLnL) whereas the tryptic activity was enhanced (12). Such a modulation of proteasome activity has not been observed with other proteasome inhibitors (14), and we decided to further investigate the mechanism of proteasome modulation by Ritonavir that most likely accounts for the observed cellular defects in antigen processing. Ritonavir partially protected the proteasome subunits MB-1 (X) and/or LMP7 from covalent active site modification with a vinyl sulfone inhibitor and could be nicely accommodated in the active site pockets of the homologous yeast subunit. This suggests that these proteasome subunits are the predominant targets

\* This work was supported by Swiss National Science Foundation Grant 32-53674.98, Roche Research Foundation, Novartis Foundation, and Rentenanstalt Jubiläumstiftung. The costs of publication of this article were defrayed in part by the payment of page charges. This article must therefore be hereby marked "advertisement" in accordance with 18 U.S.C. Section 1734 solely to indicate this fact.

\*\* To whom correspondence should be addressed: Kantonsspital St. Gallen, Laborforschungsabteilung, Haus 09, CH-9007 St. Gallen, Switzerland. Tel.: 41-71-494-1069; Fax: 41-71-494-6321; E-mail: lfal@ms1.kssg.ch.

<sup>1</sup> The abbreviations used are: HIV-I, human immunodeficiency virus, type I; <sup>125</sup>I-NLVS, 4-hydroxy-3-iodo-2-nitrophenyl-leucyl-leucyl-leucine vinyl sulfone; LLnL, *N*-acetyl-leucyl-leucyl-norleucinal; MCA, 7-amido-4-methylcoumarin;  $\beta$ NA,  $\beta$ -naphthylamide; LCMV, lymphocytic choriomeningitis virus; Iscove's modified Dulbecco's medium; PAGE, polyacrylamide gel electrophoresis; DHFR, dihydrofolate reductase.

for competitive inhibition by Ritonavir in accordance with our kinetic analysis. A selective block of the cell cycle in G<sub>1</sub>/S and a partial inhibition of protein degradation was found at concentrations that were ten-fold higher than those required for immunomodulation. Modulators of proteasome activity may therefore be useful for controlling antigen processing and the cytotoxic immune response.

#### MATERIALS AND METHODS

**Cell Culture**—The human lymphoblastoid cell line T2 (15) and the murine embryonal fibroblast line B8 (4) were grown in IMDM (Biomed, Geneva, Switzerland) supplemented with 10% fetal calf serum and 100 units/ml penicillin-streptomycin (Biological Industries, Beit Haemek, Israel).

**Proteasome Assays**—20 S proteasomes from B8 and T2 cells were purified and quantified as detailed elsewhere (4). 20 S proteasomes from *Saccharomyces cerevisiae* were isolated as previously described (16). Fluorogenic peptide substrates were diluted from 10 mM frozen stock solutions in *N,N*-dimethylformamide except for the 10 mM (Z)-LLE- $\beta$ NA stock solution that was prepared freshly each time in Me<sub>2</sub>SO. Assays were performed for 90 min at 37 °C in a total volume of 100  $\mu$ l of buffer E (50 mM Tris/HCl, pH 7.5, 25 mM KCl, 10 mM NaCl, 1 mM MgCl<sub>2</sub>, 1 mM dithiothreitol, 0.1 mM EDTA) containing 500 ng of purified 20 S proteasome, and fluorescence was determined with a Tecan SpectraFluor Plus plate reader at 30, 60, and 90 min after initiation of the reaction using emission and excitation wavelengths of 360 and 465 nm, respectively, for MCA and 340 and 405 nm, respectively, for  $\beta$ NA. Shown values are from 60-min incubations and were in the linear range of the reaction; triplicates were measured for all data points. For the ultrafiltration assays 100  $\mu$ M Ritonavir was added to 2.5  $\mu$ g/ml 20 S proteasomes in buffer E, and the Ritonavir was removed by three rounds of 1-h incubations at 37 °C followed by ultrafiltration at 300  $\times$  g through Centricon 100 filters. The proteasomes were brought to the original volume with buffer E, and an aliquot was used for activity determination with 100  $\mu$ M Suc-LLVY-MCA substrate.

**Viability Test**—Ritonavir (Abbott) was dissolved in methanol at a concentration of 50 mM. LLnL (Roche Molecular Biochemicals) was dissolved in Me<sub>2</sub>SO at a concentration of 5 mM. Both substances were diluted directly into complete IMDM. The final concentration of Me<sub>2</sub>SO was adjusted to 1%, and the final concentration of methanol was adjusted to 0.1%. 100  $\mu$ l of T2 cells were seeded in 96-well plates at a density of  $1 \times 10^6$ /ml for time points of incubation up to 48 h and at a density of  $2 \times 10^5$ /ml for incubation times from 48 to 96 h. 100  $\mu$ l of medium containing the diluted inhibitors Ritonavir and LLnL was added. After the indicated time points the viability was determined by trypan blue exclusion. All values are means of triplicates. The experiment was repeated two times, and identical results were obtained.

**Determination of Canavanine Resistance**—T2 cells were grown for 2 days in the presence of the indicated concentrations of Ritonavir. 100  $\mu$ l of T2 cells were seeded in 96-well plates at a density of  $1 \times 10^6$ /ml in RPMI 1640 medium containing 10% dialyzed fetal calf serum and 10 mg/l L-arginine (prepared with the Select-Amine kit from Life Technologies, Inc.) instead of 200 mg/l L-arginine in conventional RPMI 1640 medium. 100  $\mu$ l of the same medium containing canavanine at the indicated concentrations and Ritonavir was added. The plates were incubated for 24 h, and the viability was determined as described above. All values are means of triplicates. The experiment was repeated two times, and identical results were obtained.

**Flowcytometric Analysis of DNA Content**—T2 cells were cultured to a density of about  $2 \times 10^5$ /ml. To arrest cells with a 2 N DNA content, hydroxyurea was added at a final concentration of 0.76 mg/ml. Cells arrested with a 4 N DNA content were prepared with nocodazole at 3.2  $\mu$ g/ml final concentration. Ritonavir was added to the medium at the indicated concentrations as described above. After 48 h of incubation cells were harvested by centrifugation and fixed with ethanol. An aliquot of cells treated with 50  $\mu$ M Ritonavir was washed three times with medium (10 min. incubation between the centrifugation steps) and incubated for another 48 h before fixation. After fixation cells were washed two times with phosphate-buffered saline and resuspended at a density of  $1 \times 10^7$ /ml in phosphate-buffered saline. 50  $\mu$ l of 38 mM sodium citrate, pH 7.0, containing 50 mg/l propidium iodide, 50  $\mu$ l of 10 mg/ml RNase A, and 50  $\mu$ l of 400  $\mu$ g/ml propidium iodide in water was added, and the cells were incubated at 37 °C for 30 min. Analysis was done on a Becton Dickinson FACSCAN® flow cytometer with Lysis II software.

**Metabolic Labeling and Immunoprecipitation**—To determine the degradation rates of the murine cytomegalovirus protein pp89 aliquots

of  $1 \times 10^6$  B8 cells were treated for 2 days with 0, 10, or 50  $\mu$ M Ritonavir or for 30 min with 50  $\mu$ M LLnL. The cells were incubated for 30 min in Met-/Cys-deficient RPMI 1640 medium in the presence of inhibitors. After starvation the cells were incubated for 1 h in methionine-/cysteine-free medium plus 0.2 mCi/ml TranS<sup>35</sup> (ICN Biomedicals) in the presence of either Ritonavir or LLnL. After three washes with phosphate-buffered saline the cells were incubated for the indicated time points in IMDM plus inhibitors. Cells were harvested by centrifugation after detachment with calcium-/magnesium-free medium.  $1 \times 10^6$  cells were lysed in 35  $\mu$ l of lysis buffer (50 mM Tris/HCl, pH 7.8, 150 mM NaCl, 2% Triton X-100, 1 mM EDTA, 10 mM iodoacetamide, 1 mM phenylmethylsulfonyl fluoride, 1  $\mu$ M leupeptin, 1  $\mu$ M pepstatin, 0.3  $\mu$ M aprotinin).  $5 \times 10^6$  cpm aliquots of postnuclear lysates, which were taken for immunoprecipitation, were diluted in buffer A (50 mM Tris/HCl, pH 7.8, 150 mM NaCl, 0.5% Triton X-100, 1 mM EDTA, 10 mM iodoacetamide, 1 mM phenylmethylsulfonyl fluoride, 1  $\mu$ M leupeptin, 1  $\mu$ M pepstatin, 0.3  $\mu$ M aprotinin, 1 mg/ml ovalbumin). After 2 h of preclearing with protein A-Sepharose (Amersham Pharmacia Biotech), pp89 was immunoprecipitated over night with the monoclonal antibody 6-58.1 (17), and the beads were washed three times with buffer A. Precipitated proteins were separated by SDS-polyacrylamide gel electrophoresis (SDS-PAGE) and quantitated with a BAS 2000 imager (Fuji).

**Ubiquitin Protein Reference Technique**—To determine the impact of Ritonavir on the catabolism of Arg- $\beta$ -galactosidase we used the ubiquitin protein reference technique as described by Lévy *et al.* (18). Plasmids containing cDNAs for DHFR (hemagglutinin-tag)-ubiquitin-Arg- $\beta$ -galactosidase and DHFR (hemagglutinin-tag)-ubiquitin-Met- $\beta$ -galactosidase were kindly provided by Dr. F. Lévy, Lausanne, Switzerland. B8 cells were treated for 2 days with the indicated concentrations of Ritonavir. The DHFR-ubiquitin-Arg- $\beta$ -galactosidase or DHFR-ubiquitin-Met- $\beta$ -galactosidase expression constructs were transfected by calcium phosphate precipitation as described elsewhere (19). After 16 h of incubation the calcium phosphate/DNA coprecipitate was removed, and the cells were incubated for 6 h in IMDM. Cells were starved for methionine and cysteine, and pulse labeling was performed in Met-/Cys-deficient medium containing 0.5 mCi/ml TranS<sup>35</sup> label for the indicated time points. After the labeling the dishes containing cells were transferred to ice. The cells were washed three times with ice-cold phosphate-buffered saline and lysed with lysis buffer directly in the culture dish on ice for 30 min. Preclearing and immunoprecipitation were performed as described above, except that the antibodies Gal-13 (anti  $\beta$ -galactosidase, Sigma) and F-7 (anti HA-tag, Santa Cruz Biotechnology) were used.

**Labeling of Proteasomes with <sup>125</sup>I-NLVS**—Proteasomes were isolated from the mouse lymphoblastoid cell line EL-4 and were incubated with  $1.8 \times 10^4$  Bq/ml <sup>125</sup>I-NLVS and various concentrations of Ritonavir for 2 h at 37 °C as previously described (20). The labeling reaction was quenched by addition of 4  $\times$  SDS sample buffer, and the samples were analyzed by SDS-PAGE and autoradiography.

**Modeling**—We have performed FlexX (21) calculations to predict the potential binding mode of Ritonavir to the chymotryptic site of the yeast 20 S proteasome. FlexX requires the definition of the active site of the protein. We therefore took the x-ray structure (22) complexed with LLnL, removed the inhibitor, and defined the active site within a sphere of radius of 25.0 Å around Thr 1 of subunit  $\beta$ 5 (PRE2). The three-dimensional structure of Ritonavir (23) was built with Sybyl 6.3 (Tripos Associates, St. Louis, MO) modeling software. Correct atom types, stereocenters, hybridization states, and bond types were defined with respect to the Sybyl mol2 file format. Formal charges were assigned to each atom, and an energy minimization was performed using the Tripos force field. Because FlexX samples the conformational space of the ligand on the basis of the Mimuba approach (24) bond lengths and bond angles are kept unchanged during the docking calculation. Therefore the reasonable minimized geometry should be useful. The selection of the anchor fragment (25) was done automatically by using the "AUTODOCK" command. No refinement calculations were performed after the FlexX run.

#### RESULTS

Previously we have shown that the treatment of cells with 100  $\mu$ M Ritonavir led to an accumulation of high molecular weight ubiquitin protein conjugates, which were about 30% less abundant compared with amounts obtained after treatment with 100  $\mu$ M lactacystin or LLnL (12). The induced degradation of I $\kappa$ B $\alpha$ , a well characterized proteasome substrate, was inhibited at 100  $\mu$ M Ritonavir suggesting that Ritonavir

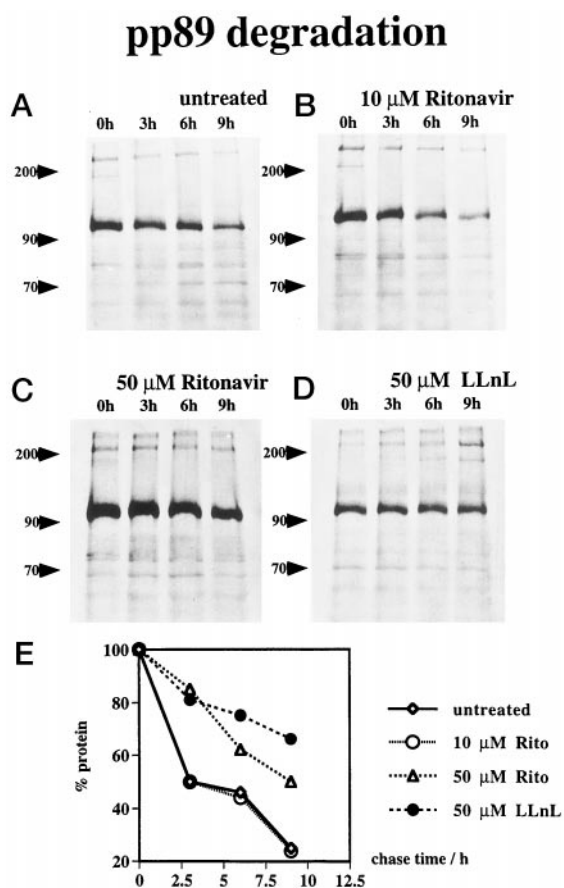


**FIG. 1. Ritonavir inhibits the degradation of the mouse cytomegalovirus pp89 protein.** B8 mouse fibroblast cells endogenously expressing pp89 were incubated with 0 (A), 10 (B), or 50  $\mu$ M Ritonavir (C) for 2 days or with 50  $\mu$ M LLnL for 1 h (D). After this pretreatment the degradation of the pp89 protein was investigated by metabolic pulse labeling for 1 h followed by pp89 immunoprecipitation and SDS-PAGE after 0, 3, 6, and 9 h of chase in the presence of inhibitors. *Panel E* shows a plot of the relative amounts of pp89 (as percents) after quantitation of radioactivity in pp89 bands (at about 90 kDa) on a phosphorimager. *Rito*, Ritonavir.

inhibited cellular protein degradation by the proteasome at least to a certain degree (12). To further investigate this issue we studied the effect of Ritonavir on the degradation of a viral antigen, a typical N-terminal rule substrate, and misfolded proteins.

**Inhibition of Protein Degradation by Ritonavir**—The immediate early protein of the mouse cytomegalovirus pp89 is processed for major histocompatibility complex class I restricted antigen presentation in a proteasome-dependent manner.<sup>2</sup> We therefore followed the pp89 protein in a pulse-chase experiment to test whether its degradation was affected by Ritonavir (Fig. 1). Ritonavir inhibited pp89 degradation to an extent comparable to LLnL at a concentration of 50  $\mu$ M but it had no effect at a concentration of 10  $\mu$ M. In contrast to the proteinolysis of I $\kappa$ B $\alpha$  and pp89, the degradation of the N-end rule substrate Arg- $\beta$  galactosidase was not changed in its metabolic stability by 10 or 50  $\mu$ M Ritonavir (Fig. 2). Rather than performing pulse-chase experiments we have applied the ubiquitin protein reference technique (18) to monitor Arg- $\beta$  galactosidase accumulation after cleavage from a DHFR-ubiquitin-Arg- $\beta$  galactosidase precursor protein. It is an advantage of this method that the accumulation of Arg- $\beta$  galactosidase during continuous labeling can be compared with the accumulation of the

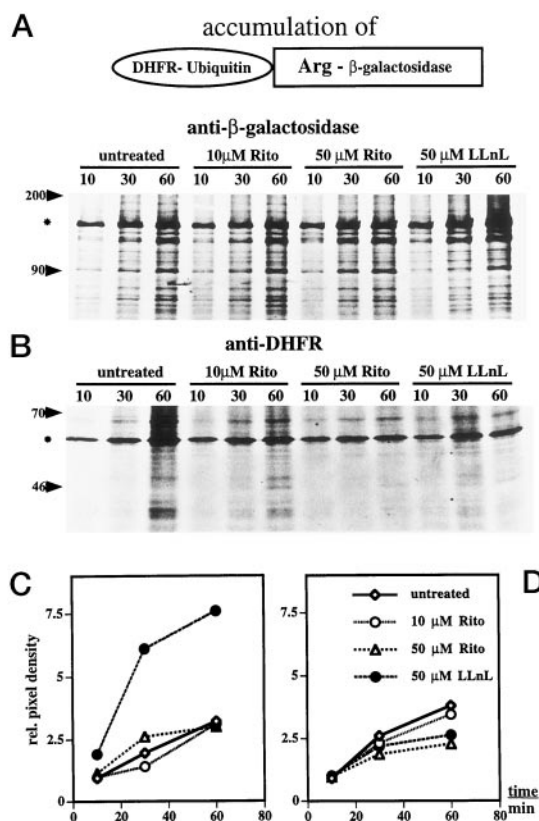


**FIG. 2. Ritonavir does not inhibit the degradation of Arg- $\beta$ -galactosidase.** B8 cells expressing the fusion protein DHFR-ubiquitin-Arg- $\beta$ -galactosidase were treated with 0, 10, or 50  $\mu$ M Ritonavir for 2 days or with LLnL for 1 h. The cells were pulse-labeled for 10, 30, and 60 min. The two parts of the fusion protein, Arg- $\beta$ -galactosidase (*panel A*) and DHFR-ubiquitin (*panel B*), which are generated by an endogenous ubiquitin C-terminal hydrolase, were immunoprecipitated and separated by SDS-polyacrylamide gel electrophoresis. The asterisks indicate the position of the respective proteins, and the arrowheads show the position of marker proteins. The amount of radioactivity in Arg- $\beta$ -galactosidase bands (*panel C*) and DHFR-ubiquitin bands (*panel D*) is plotted versus the time of pulse. *Rito*, Ritonavir.

metabolically stable DHFR ubiquitin protein, which is produced in equimolar amounts. The fact that LLnL but not Ritonavir led to an increase in Arg- $\beta$  galactosidase accumulation suggests that the extent of inhibition of proteasomal protein degradation by Ritonavir varies between different protein substrates.

As the proteasome is responsible for the removal of misfolded proteins we finally determined the effect of Ritonavir on the viability of cells that were treated with the arginine analogue canavanine (26, 27). Consistent with an inhibition of the proteasome the loss in the viability of T2 lymphoblastoid cells due to canavanine treatment was markedly enhanced by the simultaneous administration of Ritonavir in a dose-dependent manner (data not shown). As a loss in viability was already apparent at a Ritonavir concentration of 5  $\mu$ M this suggests that the proteasome was already partially inhibited at this low concentration, which we previously showed to affect antigen presentation (12).

**Ritonavir Induces a Cell Cycle Arrest in  $G_1$** —To determine the effect of Ritonavir on cell viability under normal conditions we incubated T2 cells with titrated amounts of Ritonavir and LLnL. Whereas the proteasome inhibitor LLnL killed T2 cells in culture within 24 h at a concentration of 10  $\mu$ M we saw no effect on T2 viability or proliferation at Ritonavir concentrations up to 25  $\mu$ M. At a concentration of 50  $\mu$ M Ritonavir led to a stop in proliferation, but cells remained viable according to

<sup>2</sup> G. S., unpublished observation.

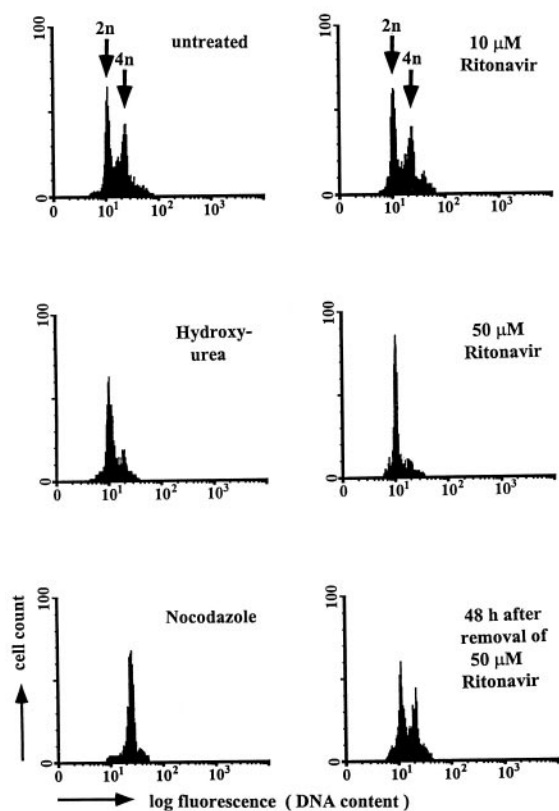


FIG. 3. **Ritonavir causes a cell cycle arrest in G<sub>1</sub>/S.** Shown are flow-cytometric analyses of propidium iodide-stained nuclei; DNA contents of 2 and 4 N are indicated by arrows. Cells were treated for 48 h as indicated: untreated, treated with hydroxyurea as G<sub>1</sub>/S phase control (2 N), treated with nocodazole as control for mitotic arrest (4 N), treated with 10 and 50  $\mu$ M Ritonavir, and treated with 50  $\mu$ M Ritonavir followed by incubation for additional 48 h in the absence of Ritonavir.

trypan blue exclusion for several days and resumed proliferation after removal of Ritonavir. As the proteasome inhibitor LLnL leads to cell cycle arrest at the G<sub>1</sub>/S boundary, in the S phase, or in mitosis (28) we examined how Ritonavir would affect cell cycle progression. Interestingly, the treatment of unsynchronized T2 cells (Fig. 3) or B8 cells (not shown) with 50  $\mu$ M Ritonavir for 48 h led to a selective and reversible arrest of the cell cycle in G<sub>1</sub> with a DNA content of 2 N as determined by flow cytometric analysis. For control of DNA content cells were either left untreated or were arrested in the S phase by hydroxyurea (2n) or in mitosis by nocodazole (4 N). At a concentration of 10  $\mu$ M Ritonavir we did not observe any effect on cell cycle progression. A specific cell cycle arrest would be consistent with a selective block in the degradation of certain proteins (cyclin-dependent kinase inhibitors, cyclins, etc.) specifically required for G<sub>1</sub>/S progression.

**Titration of Ritonavir and Substrate Concentrations**—As a first approach to study the mechanism how Ritonavir modulates proteasome activity we studied the hydrolysis of fluorogenic peptide substrates by 20 S proteasomes isolated from B8 mouse fibroblasts. The fluorogenic substrates Suc-LLVY-MCA, Bz-VGR-MCA, and (Z)-LLE- $\beta$ NA, which are frequently used to respectively monitor the chymotrypsin-like, trypsin-like, and peptidylglutamyl peptide-hydrolyzing activity of the proteasome were measured. The substrate (Z)-GGL-MCA may also be cleaved by the chymotrypsin-like activity, but as this substrate behaved quite differently from Suc-LLVY-MCA in earlier studies about the effects of interferon- $\gamma$ -inducible proteasome subunits (4) we also included it in our study.

First proteasome activity was measured at titrated concen-

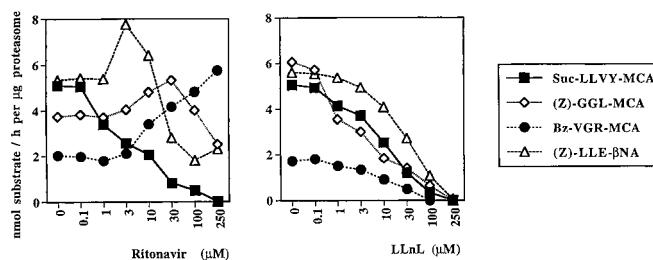


FIG. 4. **The inhibition of proteasomal hydrolysis of four fluorogenic substrates by Ritonavir and LLnL.** The cleavage activity of isolated 20 S proteasomes from murine B8 fibroblast cells is plotted against the concentration of inhibitors. The concentrations of fluorogenic substrates were left constant: 100  $\mu$ M Suc-LLVY-MCA, 100  $\mu$ M (Z)-GGL-MCA, 400  $\mu$ M Bz-VGR-MCA, and 200  $\mu$ M (Z)-LLE- $\beta$ NA. The activities are calculated from MCA measurements 60 min after initiation of digests when the reaction is in linear progression. Displayed values are the means of triplicates with S.E. of <5% for all data points.

tration of both Ritonavir and LLnL (Fig. 4). In contrast to LLnL, which similarly inhibits the hydrolysis of the four tested substrates in a concentration-dependent manner, Ritonavir shows a comparable inhibition only for the Suc-LLVY-MCA substrate with an IC<sub>50</sub> value of 3  $\mu$ M. The hydrolysis of (Z)-GGL-MCA and (Z)-LLE- $\beta$ NA was increased at Ritonavir concentrations of 3  $\mu$ M and 30  $\mu$ M, respectively, and was slightly reduced at higher concentrations. The trypsin-like activity, in contrast, was consistently enhanced in a dose-dependent manner from 10 to 250  $\mu$ M of Ritonavir. This modulation of proteasome activities by Ritonavir was highly reproducible with three independent preparations of 20 S proteasomes from B8 mouse fibroblasts and was identical for human 20 S proteasomes isolated from T2 lymphoblastoid cells (not shown). The inhibition of the proteasomal chymotrypsin-like activity was reversible as full activity was recovered upon removal of Ritonavir by ultrafiltration. Moreover, the peptide analogon Ritonavir remained unaltered during incubation with 20 S proteasomes as determined by reverse phase high pressure liquid chromatography analysis (data not shown).

Next we measured proteasome activity at three fixed concentrations of Ritonavir and increasing concentrations of the four fluorogenic substrates (Fig. 5). For the Suc-LLVY-MCA substrate we observed a proportional increase of MCA production with increasing concentrations of substrate at 1  $\mu$ M but not at 10  $\mu$ M Ritonavir suggesting that at low Ritonavir concentration this substrate can outcompete the modulator. Thus Ritonavir may act as a competitive inhibitor for the chymotrypsin-like activity. Interestingly, the enhancement of the trypsin-like activity by Ritonavir was not apparent anymore at high concentrations of the substrate Bz-VGR-MCA suggesting that this substrate also competes with Ritonavir for binding to a site that enhances the tryptic activity and that cannot be identical to an active site responsible for the trypsin-like activity.

**Ritonavir Protects the Proteasome Subunit MB-1 (X) and/or LMP7 from Covalent Modification by the Vinyl Sulfone Inhibitor NLVS**—We aimed at identifying the proteasome subunit(s) that are able to bind Ritonavir. As Ritonavir does not covalently bind to the proteasome a direct labeling of proteasome subunits with radiolabeled Ritonavir and electrophoretic analysis seems to be impossible. Our kinetic analysis suggests that Ritonavir competes with the Suc-LLVY-MCA substrate for binding to the active site of the chymotrypsin activity of the proteasome. Hence we tested whether Ritonavir would be able to protect proteasome subunits from covalent modification by the active site vinyl sulfone inhibitor <sup>125</sup>I-NLVS. This radioactively labeled proteasome inhibitor was previously shown to covalently bind to the active site-bearing subunits of mouse or

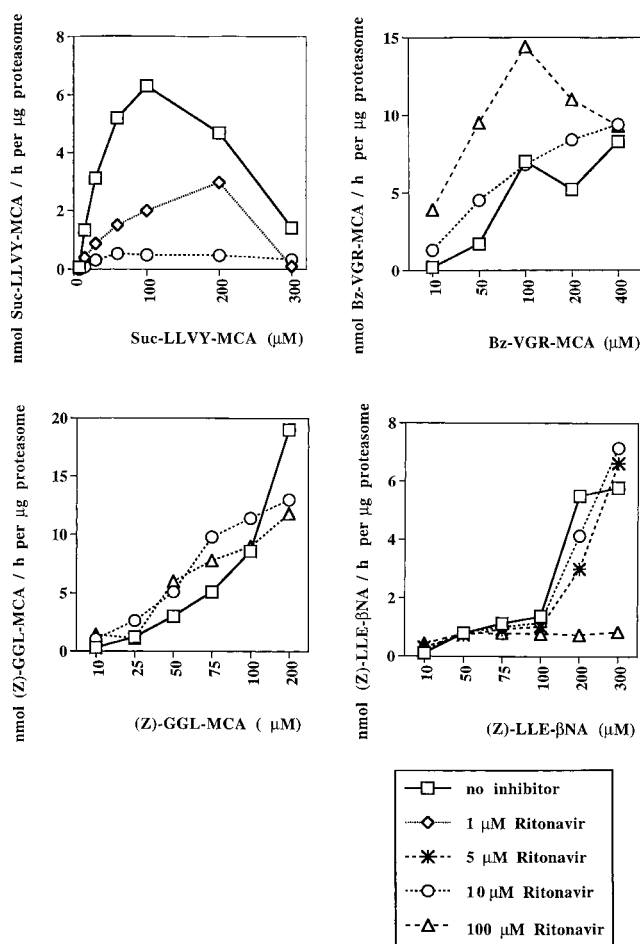


FIG. 5. The influence of substrate concentration on proteasome modulation by Ritonavir. The experimental assessment of proteasome activities in the presence of fixed concentrations of Ritonavir as indicated (0, 1, 10, or 100  $\mu\text{M}$ ) was performed as described in the legend to Fig. 4. The data represent means of triplicates with S.E. of <5% for all data points.

human proteasomes, which allows electrophoretic identification of the respective subunits (20, 29). Ritonavir partially protected the subunits LMP7 or MB-1 (X) at a concentration of 100  $\mu\text{M}$  whereas no protection of LMP2, Z, MECL-1, or Y was observed (Fig. 6). No protection was detected at lower concentrations of Ritonavir, which is most likely due to the fact that Ritonavir is a reversible competitive inhibitor that will eventually be replaced by a covalent inhibitor like  $^{125}\text{I}$ -NLVS. This result strongly suggests that the proteasome subunits LMP7 and/or MB-1 (X) are the predominant subunits for competitive active site inhibition by Ritonavir.

**Three-dimensional Modeling of Ritonavir Bound to the Yeast Proteasome Subunit PRE2**—A three-dimensional structure of mammalian 20 S proteasomes at high resolution, which could have been used to test whether Ritonavir would fit in the  $\text{P}_1/\text{P}_3$  binding pockets of the proteasome subunits LMP7 or MB-1 (X) has not yet been obtained. However, as the high resolution structure of the *S. cerevisiae* 20 S proteasome is known (22), and as Ritonavir also inhibited the chymotryptic activity of the yeast 20 S proteasome (data not shown) we performed FlexX calculations to predict whether Ritonavir can bind in the active center of the yeast PRE2 subunit that is homologous to LMP7 and MB-1 (X). Indeed, the calculation performed as outlined under "Materials and Methods" predicted that Ritonavir should inhibit the chymotryptic activity. The thirty best inhibitor positions are very well clustered in the active center of

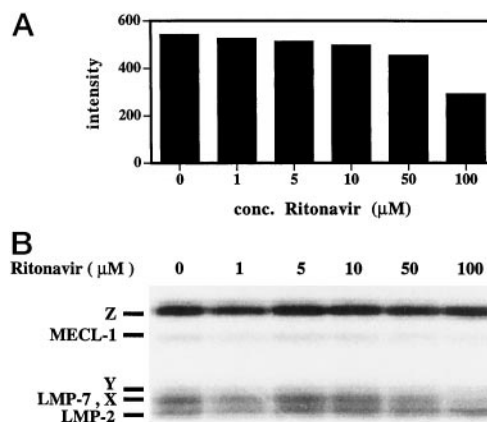


FIG. 6. Ritonavir protects the subunits LMP7 or MB-1 (X) from covalent modification by the proteasome inhibitor  $^{125}\text{I}$ -NLVS. A densitometric evaluation of the LMP7/MB-1 (X) band normalized to the density of the Z band is shown in panel A. Proteasomes isolated from EL-4 cells were incubated with indicated concentrations of Ritonavir and  $^{125}\text{I}$ -NLVS for 2 h and were subsequently analyzed by 12.5% SDS-PAGE and autoradiography (panel B).

PRE2 with predicted binding energies ranging from  $-34.44$  to  $-33.40$  kJ/mol. Fig. 7 shows the highest ranking result of the docked Ritonavir (colored white) superimposed with the cyan colored inhibitor LLnL. Ritonavir fills the gap between the strands similar to LLnL with the hydrophobic side chain at  $\text{P}_1$  projecting into the  $\text{S}_1$  pocket like the norleucinal side chain. The same holds true for the side chains in  $\text{P}_2$  and  $\text{P}_3$ . The urea unit of Ritonavir is in contact with the adjacent PRS3 subunit and is hydrogen-bonded to Asp 114. Taken together, the docking results are in accordance with the experimental evidence that Ritonavir is a competitive inhibitor of the chymotryptic activity of the 20 S proteasome.

#### DISCUSSION

The aim of this study was to investigate how Ritonavir acts as a modulator of proteasome activity and to determine the effects of this modulation on cellular functions of the proteasome. At therapeutically relevant concentrations (5  $\mu\text{M}$ ) at which immune modulation was observed Ritonavir did not affect proliferation or cell cycle progression but led to an increase in the sensitivity to canavanine. At higher concentrations of Ritonavir (50  $\mu\text{M}$ ) a selective inhibition of intracellular protein degradation and a reversible arrest of the cell cycle in the  $\text{G}_1/\text{S}$  phase were observed. A kinetic analysis suggested that Ritonavir is a reversible and competitive inhibitor of the proteasomal chymotrypsin-like activity and a positive effector of the trypsin-like activity. Ritonavir partially protected the proteasome subunit MB-1 (X) and/or LMP7 from covalent modification by the proteasome inhibitor  $^{125}\text{I}$ -NLVS and could be nicely accommodated in the active site pockets of the homologous yeast subunit, which is consistent with the kinetic analysis.

Because Ritonavir inhibited the hydrolysis of the Suc-LLVY-MCA substrate most potently this result suggests that the subunits MB-1 (X) or LMP7 are the predominant subunits that account for the chymotrypsin-like activity defined by this substrate. This notion is supported by mutagenesis experiments in *S. cerevisiae* where the inactivation of the PRE2 subunit, which is homologous to the mammalian subunits MB-1 (X) and LMP7, led to a selective elimination of the chymotrypsin-like activity (30). The site-directed inactivation of MB-1 or LMP7 in mammalian cells has not yet been reported. However, a study employing a panel of different vinyl sulfone inhibitors also showed that the potency in the inhibition of the chymotrypsin-like

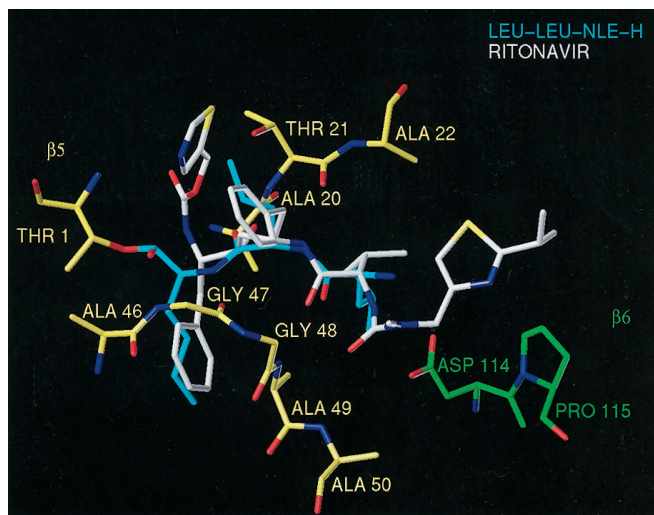


FIG. 7. Model of Ritonavir and LLnL bound in the active center of the PRE2 subunit. Shown is the highest ranking result of FlexX calculations as described under "Materials and Methods." Ritonavir is depicted in white, LLnL in cyan, residues of the PRE2 subunit ( $\beta 5$ ) are in yellow, and residues of the PRS3 subunit ( $\beta 6$ ) are in green.

activity of mouse proteasomes correlated with their ability to protect the subunits MB-1 (X) and LMP7 from covalent modification by radioactive inhibitors of the same class (20).

Although a number of proteasome inhibitors that are, at least to some extent, selective for the chymotrypsin-like activity have been described (14), a modifier of proteasome activity that inhibits one activity (chymotrypsin-like) and simultaneously enhances a second activity (trypsin-like) has not yet been described. This enhancement, which is most prominent at an intermediate concentration of the Bz-VGR-MCA substrate (Fig. 5) cannot be attributed to binding to the trypsin-like active site that, according to a recent analysis by Salzman *et al.*, (31) is located at the N terminus of the MC14 subunit. From the present data we cannot discriminate whether the Ritonavir-binding site responsible for enhancing the tryptic activity is another active site of the 20 S proteasome that allosterically activates the tryptic activity or an undiscovered modifier site at another location of the proteasome, and we are currently addressing this question experimentally.

How does a modulation of proteasome activity *in vitro* affect proteasome functions in the intact cell? The accumulation of ubiquitin conjugates and the inhibition of the LPS-induced degradation of I $\kappa$ B $\alpha$  (12) are typical consequences of proteasome inhibition suggesting that housekeeping functions of the proteasome are inhibited in cells treated with 100  $\mu$ M Ritonavir. This result indicates that the chymotrypsin-like activity of the proteasome that is inhibited to 90% at this concentration is indispensable for proliferation of cells and the intracellular degradation of I $\kappa$ B $\alpha$ , MCMV pp89, misfolded proteins, and bulk ubiquitin conjugates. Moreover, it is apparent that an increase in the trypsin-like activity cannot compensate for this inhibition. The finding that a treatment of cells with 50  $\mu$ M Ritonavir did not inhibit the degradation of the well defined proteasome substrate Arg- $\beta$ -gal was somewhat surprising. Apparently, at this concentration Ritonavir is unable to halt the degradation of some very short lived proteins. Whether this means that the degradation of some proteins is less amenable to selective proteasome inhibition than others is currently being tested among a panel of other protein substrates of the proteasome in our laboratory.

The proteasome is responsible for the programmed destruction of many key regulatory proteins involved in cell cycle control. The peptide aldehyde inhibitor LLnL, which has been

shown to bind to all active sites of the eukaryotic proteasome and which similarly affects the chymotrypsin-like, trypsin-like, and peptidylglutamyl peptide-hydrolyzing activities of the proteasome (Fig. 1), arrests the cell cycle of unsynchronized Chinese hamster ovary cells both in mitosis and the early S phase (28). In contrast, Ritonavir led to a selective cell cycle arrest of unsynchronized cells at G<sub>1</sub>/S. Interestingly, lactacystin, which also inhibits the chymotrypsin-like activity of the 20 S proteasome much more potently than the trypsin-like or peptidylglutamyl peptide-hydrolyzing activities (32) and which in yeast proteasomes bound selectively to the PRE2 subunit (*i.e.* the MB-1 (X) homologue), also led to a cell cycle arrest in G<sub>1</sub>/S (33). This could suggest that in a situation where the chymotrypsin-like activity of the proteasome becomes limiting, cell cycle regulators that need to be degraded for passing the G<sub>1</sub>/S checkpoint accumulate faster than regulators of G<sub>2</sub>/M or mitotic checkpoints. Clearly, a phase-selective arrest of the cell cycle as a consequence of proteasome modulation through Ritonavir is consistent with a substrate selectivity in affecting protein degradation.

Although our results collectively support that Ritonavir is a modulator of proteasome activity *in vivo*, it is difficult to experimentally establish that the observed effects on antigen processing and cell metabolism can exclusively be attributed to the modulation of proteasome activity. We do not know of proteases other than the HIV-1 protease and the proteasome that would be inhibited to a significant extent at a concentration of 5–10  $\mu$ M Ritonavir. Leucine aminopeptidase, which is inducible by interferon- $\gamma$  and which has been implied in antigen processing (34), is, at least, not inhibited by Ritonavir.<sup>2</sup> However, as unidentified proteases may be involved in antigen processing we cannot rule out that their inhibition could contribute to the observed clinical and experimental phenotypes. Proof of the principle that the selective inhibition of one but not other proteasome subunits can influence antigen processing without affecting cell viability or proliferation has recently been obtained by the functional inactivation of the subunits  $\Delta$  and LMP2 in mutant cell lines (19). Selective inhibitors or modulators of proteasome activity such as Ritonavir may thus be applied to modulate the cytotoxic immune response for immunosuppressive therapy in organ transplantation or for the treatment of autoimmune diseases.

#### REFERENCES

- Moyle, G., and Gazzard, B. (1996) *Drugs* **51**, 701–712
- Erickson, J., Neidhart, D. J., VanDrie, J., Kempf, D. J., Wang, X. C., Norbek, D. W., Plattner, J. J., Rittenhouse, J. W., Turon, M., Wideburg, N., Kohlbrenner, W. E., Simmer, R., Helfrich, R., Paul, D. A., and Knigge, M. (1990) *Science* **249**, 527–533
- Coux, O., Tanaka, K., and Goldberg, A. L. (1996) *Annu. Rev. Biochem.* **65**, 801–847
- Groettrup, M., Ruppert, T., Kuehn, L., Seeger, M., Standera, S., Koszinowski, U., and Kloetzel, P. M. (1995) *J. Biol. Chem.* **270**, 23808–23815
- Kuckelkorn, U., Frentzel, S., Kraft, R., Kostka, S., Groettrup, M., and Kloetzel, P.-M. (1995) *Eur. J. Immunol.* **25**, 2605–2611
- Niedermann, G., Butz, S., Ihlenfeldt, H. G., Grimm, R., Lucchiari, M., Hoschützky, H., Jung, G., Maier, B., and Eichmann, K. (1995) *Immunity* **2**, 289–299
- Nussbaum, A. K., Dick, T. P., Keilholz, W., Schirle, M., Stevanovic, S., Dietz, K., Heinemeyer, W., Groll, M., Wolf, D. H., Huber, R., Rammensee, H. G., and Schild, H. (1998) *Proc. Natl. Acad. Sci. U. S. A.* **95**, 12504–12509
- Dick, T. P., Nussbaum, A. K., Deeg, M., Heinemeyer, W., Groll, M., Schirle, M., Keilholz, W., Stevanovic, S., Wolf, D. H., Huber, R., Rammensee, H. G., and Schild, H. (1998) *J. Biol. Chem.* **273**, 25637–25646
- Deeks, S. G., Smith, M., Holodniy, M., and Kahn, J. O. (1997) *JAMA* **277**, 145–153
- Perrin, L., and Telenti, A. (1998) *Science* **280**, 1871–1873
- Kempf, D. J., Marsh, K. C., Denissen, J. F., McDonald, E., Vasavanonda, S., Plentge, C. A., Green, B. E., Fino, L., Park, C. H., Kong, X., Wideburg, N. E., Saldivar, A., Ruiz, L., Kati, W. M., Sham, H. L., Robins, T., Stewart, K. D., Hsu, A., Plattner, J. J., Leonard, J. M., and Norbeck, D. (1995) *Proc. Natl. Acad. Sci. U. S. A.* **92**, 2484–2488
- André, P., Groettrup, M., Klenerman, P., deGiuli, R., Booth, B. L., Cerundolo, V., Bonneville, M., Jotereau, F., Zinkernagel, R. M., and Lotteau, V. (1998) *Proc. Natl. Acad. Sci. U. S. A.* **95**, 13120–13124
- Groettrup, M., Soza, A., Kuckelkorn, U., and Kloetzel, P. M. (1996) *Immunol.*

- Today* **17**, 429–435
14. Groettrup, M., and Schmidtke, G. (1999) *Drug Discov. Today* **4**, 63–71
  15. Salter, R. D., and Cresswell, P. (1986) *EMBO J.* **5**, 943–949
  16. Achstetter, T., Ehmann, C., Osaki, A., and Wolf, D. H. (1984) *J. Biol. Chem.* **259**, 13344–13348
  17. Keil, G. M., Fibl, M. R., and Koszinowski, U. (1985) *J. Virol.* **54**, 422–428
  18. Lévy, F., Johnsson, N., Rümenapf, T., and Varshavsky, A. (1996) *Proc. Natl. Acad. Sci. U. S. A.* **93**, 4907–4912
  19. Schmidtke, G., Eggers, M., Ruppert, T., Groettrup, M., Koszinowski, U., and Kloetzel, P. M. (1998) *J. Exp. Med.* **187**, 1641–1646
  20. Bogyo, M., Shin, S., McMaster, J. S., and Ploegh, H. L. (1998) *Chem. Biol.* **5**, 307–320
  21. Rarey, M., Kramer, B., Lengauer, T., and Klebe, G. (1996) *J. Mol. Biol.* **261**, 470–489
  22. Groll, M., Ditzel, L., Löwe, J., Sato, D., Bochtler, M., Bartunik, H. D., and Huber, R. (1997) *Nature* **386**, 463–471
  23. Ohata, Y., and Shinkai, I. (1997) *Bioorg. Med. Chem.* **5**, 461–462
  24. Klebe, G., and Mietzner, T. (1994) *J. Comput. Aided Mol. Des.* **8**, 583–606
  25. Rarey, M., Kramer, B., and Lengauer, T. (1997) *J. Comput. Aided Mol. Des.* **11**, 369–384
  26. Ciechanover, A., Finley, D., and Varshavsky, A. (1984) *Cell* **37**, 57–66
  27. Rock, K. L., Gramm, C., Rothstein, L., Clark, K., Stein, R., Dick, L., Hwang, D., and Goldberg, A. L. (1994) *Cell* **78**, 761–771
  28. Sherwood, S. W., Kung, A. L., Roitelman, J., Simoni, R. D., and Schimke, R. T. (1993) *Proc. Natl. Acad. Sci. U. S. A.* **90**, 3353–3357
  29. Bogyo, M., McMaster, J. S., Gaczynska, M., Tortorella, D., Goldberg, A. L., and Ploegh, H. (1997) *Proc. Natl. Acad. Sci. U. S. A.* **94**, 6629–6634
  30. Heinemeyer, W., Fischer, M., Krimmer, T., Stachon, U., and Wolf, D. H. (1997) *J. Biol. Chem.* **272**, 25200–25209
  31. Salzmann, U., Kral, S., Braun, B., Standera, S., Schmidt, M., Kloetzel, P. M., and Sijts, A. (1999) *FEBS Lett.* **454**, 11–15
  32. Fenteany, G., Standaert, R. F., Lane, W. S., Choi, S., Corey, E. J., and Schreiber, S. L. (1995) *Science* **268**, 726–731
  33. Fenteany, G., Standaert, R. F., Reichard, G. A., Corey, E. J., and Schreiber, S. L. (1994) *Proc. Natl. Acad. Sci. U. S. A.* **91**, 3358–3362
  34. Beninga, J., Rock, K. L., and Goldberg, A. L. (1998) *J. Biol. Chem.* **273**, 18734–18742